^{239}Pu data of JENDL-3.3

Masayoshi Kawai
KEK, 1-1 Oho, Tsukuba, Ibaraki-ken 305-0801, Japan
Masayoshi.kawai@kek.jp

^{239}Pu data of JENDL-3.3 were originally evaluated in 1987. After then, fission cross sections of important heavy isotopes, ^{233}U, ^{235}U, ^{238}U, ^{239}Pu, ^{240}Pu and ^{241}Pu were simultaneously evaluated and its results were adopted for JENDL-3.3. Integral test of JENDL-3.3 made by other authors showed that JENDL-3.3 well reproduced the k-eff of Pu-fuelled FBR critical cores and thermal reactors within about 0.5%. The C/E values of F25/F49 and C28/F49 in ZPPR-9 core were 1.02 and 1.04.

1. Introduction

^{239}Pu is one of the most important nuclides of nuclear fuel of fission reactors and very high accuracy of its nuclear data is required for designing the fast breeding reactors (FBR), MOX-fueled reactors and fuel re-processing facilities. Thus, the data of ^{239}Pu were evaluated for the first version of JENDL, i.e., JENDL-1/1/. Many analyses of reactor physics experiments with JENDL-1 and ENDF/B-IV were made for MONJU and large FBR. These information was fed back to JENDL-2 evaluation/2/.

Reevaluation for JENDL-3 were made on the basis of differential data such as measured cross sections and nuclear model calculations, since there were a lot of new experimental data after completion of JENDL-2 and reactor physics calculation accuracy became higher due to applying continuous-energy Monte Carlo methods. The results of reevaluation were compiled into JENDL-3.1/3/ in 1989. Integral test was made and showed that there were not any serious problems in ^{239}Pu data of JENDL-3.1. Then, slight modification has been made for JENDL-3.2 and 3.3. The followings are the history of the evaluation of ^{239}data for JENDL-3:

Evaluations of ^{239}Pu for JENDL-3.1 were made by taking into consideration of the reliability and consistency of the experimental data and by supplementing the data with the statistical model calculations in 1987. Contributions to the evaluation were as follows:

Cross sections evaluated and calculated by M. Kawai and K. Hida,
Simultaneous evaluation of fission cross section above 30 keV by Y. Kanda et al./4/
Resolved resonance parameters up to 1 keV selected by T. Yoshida,
Unresolved resonance parameters determined with ASREP code/5/ by T. Nakagawa.

For JENDL-3.2 in 1993,
Resolved resonance parameters up to 2.5 keV evaluated by Derrien./6/,
Fission spectra calculated by T. Ohsawa et al./7/

For JENDL-3.3,
Addition of direct and semi-direct capture cross sections calculated by T. Kawano,
Fission spectra above 10 MeV modified by T. Kawano et al./8/

The nuclear data evaluation and integral tests of JENDL-3.2 and 3.3 are described in the following sections.

2. Nuclear Data Evaluation

2.1 Number of prompt fission neutrons

Most of experimental data of ν_p of neutron induced fission for ^{239}Pu were measured as a ratio to ν_p for ^{252}Cf spontaneous fission or the thermal value of ^{239}Pu fission. Therefore, all experimental data and previously evaluated data were renormalized to the following standard values:

ν_p for ^{252}Cf spontaneous fission = 3.756

ν_p for ^{239}Pu fission at thermal = 2.8781 which was derived by weighted-averaging the experimental data.

The energy dependent ν_p were evaluated based on the experimental data/9-14/ except for adopting the Frehaut's evbaluation/15/ in the energy range between 10 eV and 500 eV. Below 500 eV, ν_p has energy dependence considering an effect of the strong resonance with the spin state J=1 at 0.3 eV as shown in Fig. 1. Above 500 eV, evaluated ν_p values are given by the following polynomials which were obtained by eye-guide fitting the reliable measured data:

$$
\nu_p = \begin{cases} 0.135\,En + 2.8675 & \text{for } En = 100\text{ keV} - 1.5\text{ MeV}, \\ 0.1534\,En + 2.8399 & \text{for } En = 1.5\text{ MeV} - 5.3\text{ MeV}, \\ 0.1521\,En + 2.8469 & \text{for } En = 5.3\text{ MeV} - 11.5\text{ MeV} \\ 0.1305\,En + 3.0953 & \text{for } En = 11.5\text{ MeV} - 19.6\text{ MeV} \\ 0.0902\,En + 3.885 & \text{for } En = 19.6\text{ MeV} - 30\text{ MeV..} \end{cases}
$$

2.2 Total cross section

Below 7 MeV, JENDL-2 evaluation was adopted, which were obtained by fitting the polynomials to the experiments of refs./16 -20/ with the weighted least squares method. Above 7 MeV, experimental data by Poenitz et al./21/ were adopted.

2.3 Fission cross section

There were a lot of experimental data reported from the various institutes in the world. However, it should be noted that the experimental data of Gayther/22/ at Harwell and Wagemans et al./23/ at GEEL were highly accurate and quite consistent with each other. Therefore, the fission cross sections below 30 keV were evaluated based on their data. Figure 2 compares the evaluated and measured fission cross sections between 1 keV and 100 keV. Above 30 keV, it is necessary to obtain the overall consistent evaluation for absolute measurements of ^{239}Pu fission cross sections and ratio measurements to ^{235}U fission cross section. This requirement was needed for important nuclides such as ^{233}U, ^{235}U, ^{238}U, ^{239}Pu, ^{240}Pu and ^{241}Pu. Therefore, simultaneous evaluation for JENDL-3 was made/4/ to determine the fission cross sections of these nuclides with the generalized least-squares calculation by estimating the covariance matrices of the experimental data. Recently, new simultaneous evaluation performed by Kawano et al./24/ using the SOK code was adopted to JENDL-3.3.

2.4 Capture cross section

The cross section in the energy range below 1 MeV was derived as a product of the evaluated fission cross section and α-value (ratio of capture to fission cross sections). After the measurement of high alpha value by Ryabov et al./25/, many experimental data of alpha values had been reported. However, evaluation of alpha value was made on the basis of Gwin's highly accurate data/26/ below 30 keV and by least-squares fit of the experimental data above 30 MeV. Figure 3 shows comparison of the evaluated and measured α-values in the energy region between 1 keV and 1000 keV. Above 1 MeV the results of the statistical model calculation with CASTHY and ECIS were adopted. The photon strength function was normalized in the CASTHY calculation so as to reproduce the capture cross section of 280 mb at 100 keV. The results were compiled into JENDL-3.1.

For JENDL-3.3, direct and semi-direct capture cross sections were calculated by Kawano above 500 keV. Figure 4 shows the capture cross sections up to 10 MeV.

2.5 Inelastic scattering cross sections

The compound components were calculated with the optical and statistical model code CASTHY, taking into account level fluctuation and interference effects. The fission, (n,2n), (n,3n), and (n,4n) reactions were considered as competing processes. The neutron transmission coefficients for the incident channel were generated with ECIS, whereas those for the exit channel were calculated with CASTHY using spherical optical potential parameters adopted for JENDL-2 evaluation. The direct components were calculated with coupled channel code ECIS. Eight levels of the ground state rotational band were coupled in the calculation. Deformed optical potential parameters with a derivative Woods-Saxon absorption term were taken from Arthur et al./27/ The calculated excitation functions for the first and second levels are in general agreement with the data of Haouat et al./28/ as shown in Fig. 5.

2.6 (n, 2n) and (n, 3n) cross sections

The (n, 2n) and (n, 3n) cross sections shown in Figs. 6 and 7 were calculated with a modified version of GNASH to subtract the fission components from the compound cross sections and to treat transmission coefficients of the incident and exit channels separately. The neutron transmission coefficients were generated with the optical model code ELIESE-3 and the coupled channel code ECIS, respectively, using the above-mentioned spherical and deformed potentials for the evaluation of inelastic scattering cross section. The evaluated fission cross section mentioned above was fed to GNASH as a competing process. The preequilibrium process was taken into account. Though the Kalbach's constant for preequilibrium process was adjusted, the calculated (n,2n) cross section did not reproduce so well the measured data in the lower energy region. Therefore, the measured (n,2n) cross section of Frehaut et al./29/ was adopted in place of the calculated data.

Figure 6 compares the evaluated and measured (n, 2n) cross sections. JENDL-3.3 agrees with the experimental data of Frehaut et al. and shows a slight lump at 18 MeV because the competing fission cross section of JENDL-3.2 has a shape of a shallow valley. The evaluated (n, 3n) cross section of JENDL-3.3 is based on the statistical model calculation and fairly similar to ENDF/B-VI and JEF-3.0 as shown in Fig. 7.

2.7 Resonance parameters

For JENDL-3.3, resolved resonance parameters up to 2.5 keV were adopted from the new evaluation by Derrien/6/ using the SAMMY code fitting to the experimental data. Unresolved resonance parameters were derived by Nakagawa with the ASREP code/5/, fitting to the evaluated total, fission and capture cross sections mentioned above.

3. Integral test of ^{239}Pu data of JENDL-3

3.1 Benchmark cores analyzed with MVP code

Integral test of JENDL-3.2 and JENDL-3.3 was made by Takano et al./30/ of JAERI, analyzing various critical experiments of FBR benchmark cores of ^{233}U, ^{235}U and Pu by using the continuous energy Monte Carlo code MVP. Effective neutron multiplication factor, k-eff, was calculated within the statistical errors of 0.02%. Since modification of important quantities of JENDL-3.2, such as fission cross section of ^{233}U and ^{235}U, total cross sections of iron etc. have been made for JENDL-3.3, improvement of k-eff of JENDL-3.3 was shown for the ^{233}U and ^{235}U cores compared to JENDL-3.2, but almost the same results were obtained for plutonium cores. The results of C/E-values for k-eff for Pu cores are given in Table 1. The table shows that JENDL-3.2 and -3.3 generally reproduces the k-eff values within 0.5%, while ENDF/B-VI.5 and JEF-2.2 have worse cases showing discrepancies more than 1% from the experimental values.

Similar integral test was also made for thermal reactors. Remarkably good results for k-eff of Pu-fueled cores are given in Table 2.

Table 1 Comparison of C/E-values of k-eff for Pu benchmark cores of FBR/30/

	JENDL-3.3	JENDL-3.2	ENDF/B-VI.5	JEF-2.2
Small core				
JEZBEL	0.9971	0.9972	0.9982	0.9971
JEZBEL-Pu	1.0014	1.0015	0.9986	0.9986
FLATOP-Pu	0.9920	0.9928	1.0044	0.9896
THOR	1.0070	1.0061	1.0060	0.9806
Large core				
FCA-XVII-1	1.0013	1.0022	1.0114	1.0093
ZPPR-9,	0.9945	0.9939	1.0038	0.9972
ZPPR-13A,	0.9947	0.9938	1.0033	0.9975
JOYO-MK-II	1.0024	1.0003	1.0059	1.0100
FCA-X-2	1.0012	1.0009		

Table 2 Comparison of C/E-values of k-eff for Pu-fuel thermal cores/30/

	JENDL-3.3	JENDL-3.2	ENDF/B-VI.5	JEF-2.2
TCA-242Pu	0.9952	0.9959	0.9913	0.9930
TCA-298Pu	0.9960	0.9968	0.9927	0.9941
TCA-424Pu	0.9975	0.9978	0.9940	0.9950
TCA-555Pu	0.9977	0.9987	0.9945	0.9952

As for the reaction rate ratio in the ZPPR-9 core, F25/F49 was 1.02 and C28/F49 was 1.04 in case of JENDL-3.3, and they were 1.02 and 1.03 in case of JENDL-3.2. Good agreement of the JENDL-3.2 and JENDL-3.3 calculations with the experimental values were also obtained for doppler reactivities of UO_2 sample, sodium void reactivities and control rod worths in the FBR cores.

3.2 Integral test for fast reactors

Another integral test of JENDL-3.3 was reported by Chiba/31/ of JNC for several fast reactors: ZPPR (JUPITER cores), FCA, JOYO, MOZART and BFS with the JUPITER standard calculation scheme standing on the Bondarenko-type 70-group cross-section library, JFS-3-J3.3.

Figures 8 and 9 show comparison of the C/E values for k-eff of various fast reactor cores analyzed with

JENDL-3.2 and JENDL-3.3. JENDL-3.3 shows a trend of slight underestimation of k-eff but discrepancy from the experimental values are small. Moreover, it does not have any core dependence compared to JENDL-3.2. BFS cores should be classified into a uranium fueled one and difference between JENDL-3.2 and JENDL-3.3 is remarkable.

Discrepancies of calculated values from the experimental data are observed only in the ^{239}Pu fission rate distribution in the reflector of BFS-62-2 core. However, this discrepancy can not be caused by uncertainty of ^{239}Pu data, because BFS-62-2 is a uranium fueled core and few-group calculation likely overestimates neutron fluxes in the region outside of the core where a steep flux change occurred.

4. Conclusion

^{239}Pu data of JENDL were drastically revised from JENDL-2 to JENDL-3.1 by adopting new evaluation techniques with a simultaneous evaluation of fission cross sections with the generalized least squares method and nuclear model calculations with the combination of the CASTHY and ECIS codes. Moreover, in evaluation, reliable experimental data were selected from a lot of measured data after careful examination. For the alpha-value, JENDL-2 data were adopted to JENDL-3. This selection gave satisfactorily good results of the integral test even for early version of JENDL-3. Accordingly, for JENL-3.3, there were only modifications of the fission cross section above 30 keV due to the new simultaneous evaluation, a part of fission spectrum, a part of resolved resonance parameters evaluated by Derrien, and addition of direct and semi-direct components to the capture cross sections.

Integral tests showed that JENDL-3.3 reproduced k-eff of fast and thermal reactors within 0.5% which is a limitation of judging quality of nuclear data. The difference (which is small in case of plutonium fueled cores) in JENDL-3.2 and JENDL-3.3 results of integral tests can be attributed to other isotopes than ^{239}Pu. It should be also noted that JENDL-3.3 gives better results than ENDF/B-VI.5.

Acknowledgement:

Author is highly indebted to Dr. T. Nakagawa of JAERI providing figures of comparison of the evaluated and measured cross sections for ^{239}Pu. He also appreciates kindness of Dr. H. Takano who gave the integral test results.

References:

1) Igarasi, S. et al,: JAERI 1261 (1979) .
2) Nakagawa, T. (ed.): JAERI-M 84-103 (1984); Kikuchi, Y. et al.: J. Nucl. Sci. Technol. 22, 593 (1985).
3) Shibata, K., et al.: JAERI 1319 (1990).
4) Kanda, Y. et al.: Proc. Int. Conf. on Nuclear Data for Basic and Applied Science, 13 - 17 May 1985, Santa Fe, p.1567 (1985).
5) Kikuchi, Y. et al.: JEARI-data/code 99-025 (1999).
6) Derrien, H.: J. Nucl. Sci. Technol., 30, 845 (1993).
7) Ohsawa, T. et al.: Nucl. Phys. A665, 3 (2000).
8) Kawano, T. et al.: Phys. Rev., C63, 034601 (2001).
9) Gwin, R. et al.: Nucl. Sci. Eng., 94, 365 (1986).

10) Gwin, R. et al.: Nucl. Sci. Eng., 87, 381 (1984).
11) Soleilhac, M. et al.: Proc. of Second IAEA Conf. on Nuclear Data for Reactors, 15-19 Jun 1970, Helsinki, Finland, Vol. 2, p. 145 (1970).
12) Soleilhac, M. et al.: J. Nucl. Energy. 23. 257 (1969).
13) Nurpeisov, B. et al.: At. Energiya, 39, 199 (1975).
14) Vorodin, K.E. et al.: At. Energiya. 33. 901 (1972).
15) Frehaut, J.: NEANDC(E)-238/L (1986).
16) Uttely, C.A.: EANDC(UK)-40 (1964).
17) Schwartz, R.B. et al.: Nucl. Sci. Eng., 54, 322 (1974).
18) Foster, D.G.Jr. and Glagow, D.W.: Phys. Rev., C3, 576 (1971).
19) Smith, A.B. et al.: J. Nucl. Energy, 27, 317 (1973).
20) Nadolny, et al.: C00-3058-39, 33 (1973).
21) Poenitz, W.P. et al.: Nucl. Sci. Eng., 78, 333 (1981).
22) Gayther, D.B.: Conf. on Nuclear Cross Sections and Technology, 3-7 Mar 1975, Washington, D.C., , Vol. 2, p. 560 (1975).
23) Wagemans, C. et al.: Ann. Nucl. energy, 7, 495 (1980).
24) Kawano, T. et al.: JAERI-Research 2000-004 (2000).
25) Ryabov, Y.V. et al.: Atomnaya Energiya, 24, 351 (1968).
26) Gwin, R. et al.: Nucl. Sci. Eng., 59, 79 (1976).
27) Arthur, E.D. et al.: Nucl. Sci. Eng. 88, 56 (1984).
28) Haouat, W. et al. : Nucl. Sci. Eng., 81, 491 (1982).
29) Frehaut, J. et al.: CEA-N-2500 (1986); Proc. Int. Conf. on Nuclear Data for Basic and Applied Science, May 1985, Santa Fe, p.1561 (1985)
30) Takano, H. et al.: J. Nucl. Sci. Technol., Supplement 2, p. 847 (202).
31) Chiba, G.: http: JAERI-Conf 2003-006, p.22 (2004).

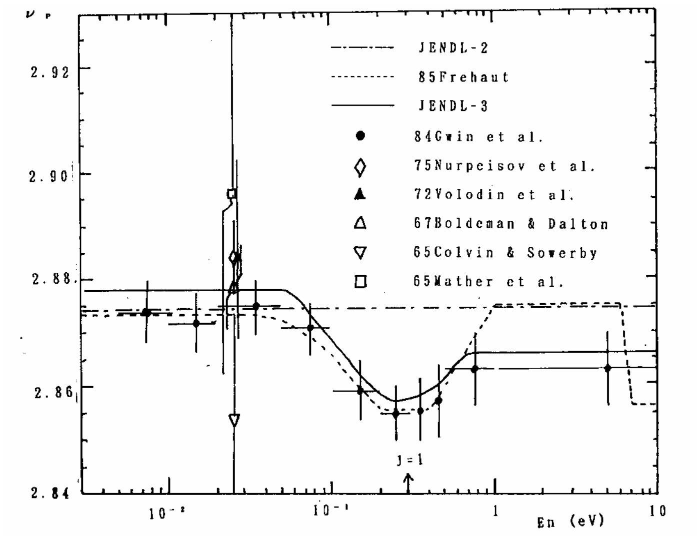

Fig. 1 Comparison of ν_p of ^{239}Pu. Effect of the strong resonance at 0.3 eV with the spin state J=1 is observed.

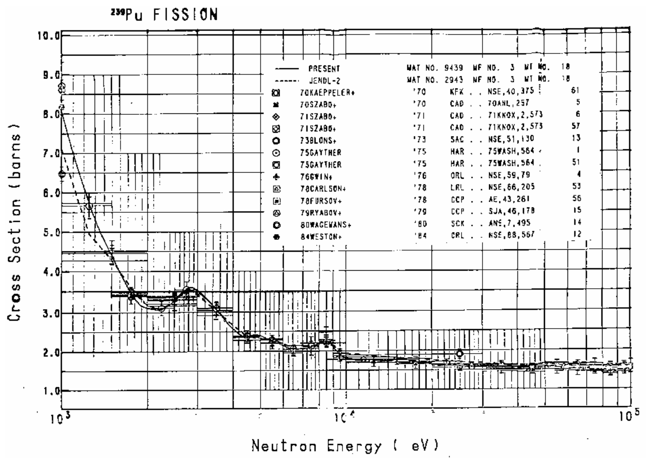

Fig. 2 Comparison of evaluated and measured fission cross sections of ^{239}Pu

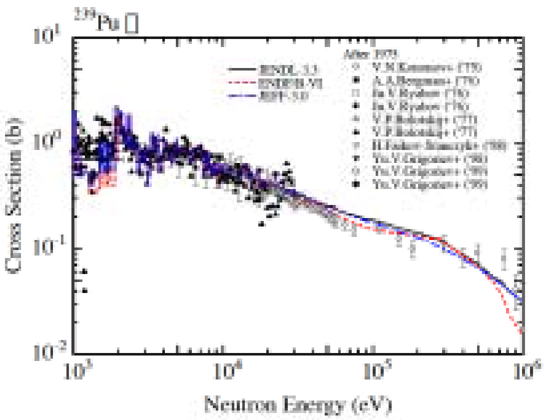

Fig. 3 Comparison of evaluated and measured α-values for ^{239}Pu.

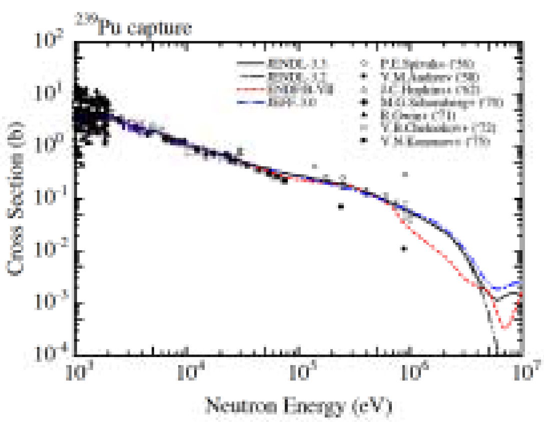

Fig. 4 Comparison of evaluated and measured capture cross sections for ^{239}Pu.

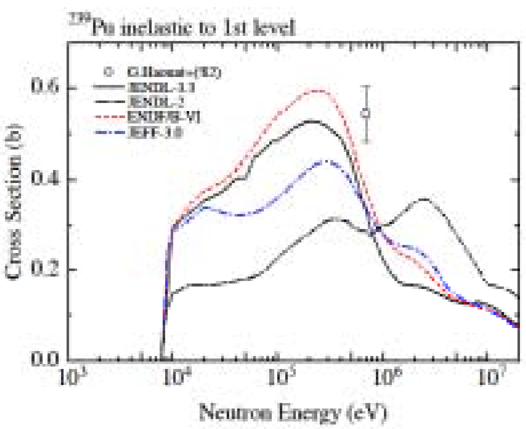

(a) First-excited state

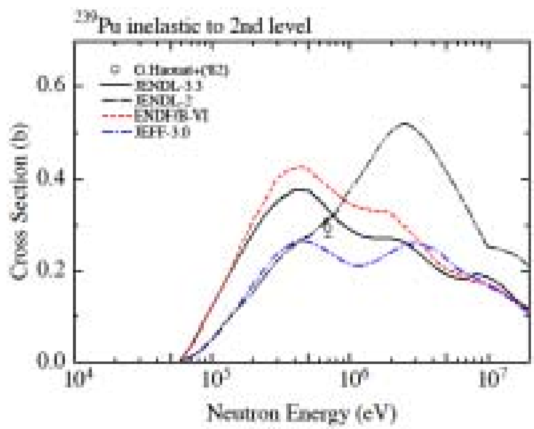

(b) Second excited state

Fig. 5 Comparison of inelastic excitation functions for ^{239}Pu.

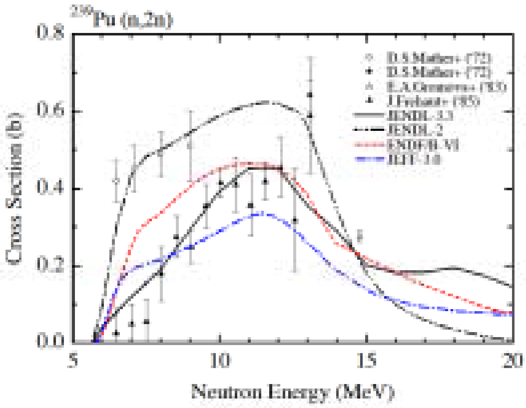

Fig. 6 Comparison of (n, 2n) cross sections

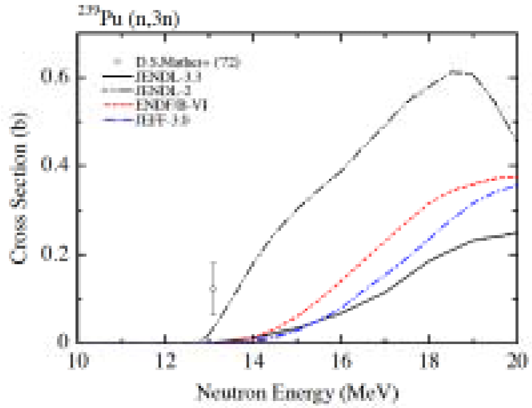

Fig. 7 Comparison of (n, 3n) cross sections

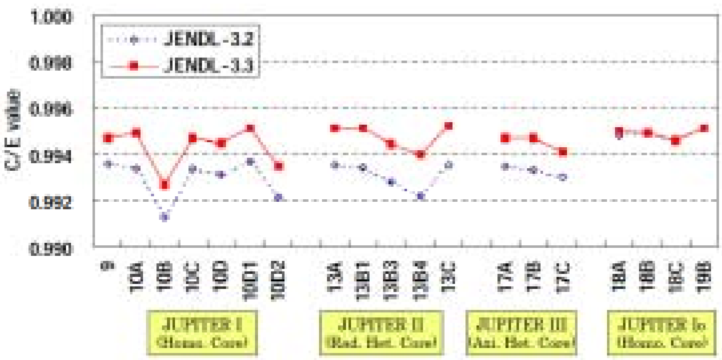

Fig. 8 C/E values of k-eff for various configuration of the JUPITER cores/31/

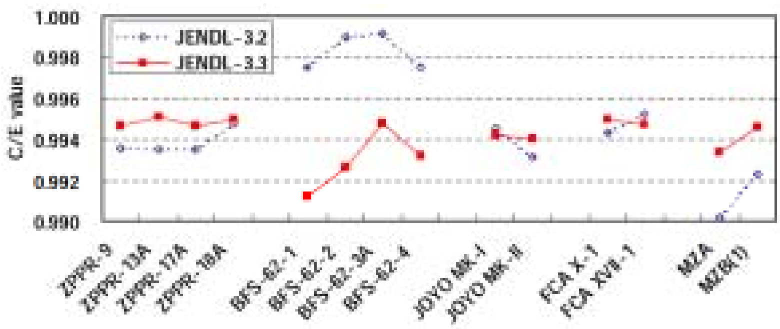

Fig. 9 C/E values of k-eff for various reactors/31/. BFS-62-1 and 62-2 are uranium-fueled.